The Influence of Flue Wall Deformation on Anode Baking Homogeneity for the Aluminum Production

Mouna Zaidani[1], Rashid K. Abu Al-Rub[2], Abdul Raouf Tajik[3], Zahid Ahmed Qureshi[4] and Tariq Shamim[5]

1. Postdoctoral Researcher
2. Department Head and Associate Professor
3. Ph.D. Student
4. MSc. Student
5. Professor

Institute Center for Energy (iEnergy), Department of Mechanical and Materials Engineering, Khalifa University of Science and Technology, Masdar Institute, Abu Dhabi, U.A.E.
Corresponding author: rabualrub@masdar.ac.ae

Abstract

In horizontal flue wall carbon baking furnaces, the flue walls consist of brick wall which are usually linked together by mortar. During service, the thermal expansion of flue walls is restrained due the presence of headwalls. This, as well as the effect of the load of the packing cokes and the anodes, promotes the deflection of the flue walls thus limits their life. The development of a 3D computational model able to take into account a large number of phenomena and parameters that play a role in the baking process and affect the flue wall aging process is then justified. In this study, we developed a 3D model that take into account the thermo-hydro-mechanical coupling due to coupled fluid flow, heat transfer and flue wall deformation. The coupled thermo-hydro-mechanical simulations were done by the finite element multi-physics commercial software COMSOL, where only a coupled flow thermal problem is solved. The mechanical problem is coupled indirectly by considering a deflected deformed flue walls. Such a 3D multi-physics modelling can be used as a powerful tool in predicting the effect of flue wall deformation on anode temperature distribution and homogeneity and thus predicting the anode baking quality. The tool may also be used to gain insights on temperature distribution adjustment as a function of the flue wall and furnace design. The main objective of this kind of investigation is to establish a flue wall deformation modes database and link it to the anode baking quality, by developing this tool, we can effectively predict the deformed flue wall reliability under varying operating conditions, and provide useful insights on enhancing the long-term structural integrity through furnace design adjustment.

Keywords: Baking process, aging, deflection, flue wall, thermo-hydro-mechanical coupling.

1. Introduction

The quality of anode used in the aluminum industry depends strongly on the baking process. In general, it is desirable to achieve a more uniform temperature inside the anode during the heating process. The flue walls in carbon bake furnaces deform over time under cyclic heating and cooling, leading to difficulties in loading/unloading anodes, and inconsistent anode baking. It is useful to regularly measure the deformations to establish the rate of deterioration and assist in the prediction of flue wall life. The aging of baking furnace, and the deformation of flue-walls and head-walls lead to non-homogeneous baking of anodes and consequently to a deterioration of the resulting anode quality [1][2][3].

Due to huge size of baking furnace and its very large time constant (in the order of months), it is not always possible to conduct physical experiments in order to determine the influence of the flue wall deformation on furnace's behavior and efficiency. The increasing interest in this topic has heightened the need for a mathematical model as a tool for predicting the influence of flue wall aging on the anode baking homogeneity. However, only a few recent investigation studies have focused on the flue wall deformation modes and their effects on the baked anode quality [4][5] .Most of the research work in this area has been focused on the process modeling considering a straight flue wall without considering the effect of flue wall deformation.

The life of carbon baking furnaces is usually limited by the deflection of its flue walls. This deflection as shown in Fig.1 is promoted principally by the action of headwalls which restrain the free thermal expansion of flue walls, and by the action of packing coke whose weight is partially supported by flue walls [6]. In a horizontal baking furnace, flue walls consist of firebricks linked together by mortar in horizontal joints. During service, the thermal expansion of flue walls is restrained due the presence of headwalls as well as the effect of the load of packing cokes and anodes that promote the deflection of the flue walls; thus, limits their service life [7][8][9].

The focus of this paper is on the development of a numerical tool that can effectively predict the furnace performance considering its deformation. Such a deformation leads to anode baking inhomogeneity, anode overbaking, hot spot formation and creates difficulties in loading and unloading of anodes in the pits. In this study, a multi-physics 3D model is developed. This model is applied to one heating section of the baking furnace in order to explore the effect of flue wall deformation on the baking quality and temperature homogeneity of the anodes. The developed computational tool can be used to explore the different flue wall deformation patterns, and their effects on the anode baking homogeneity. The tool may also be used to gain insights on temperature distribution adjustment as a function of the flue wall and furnace design.

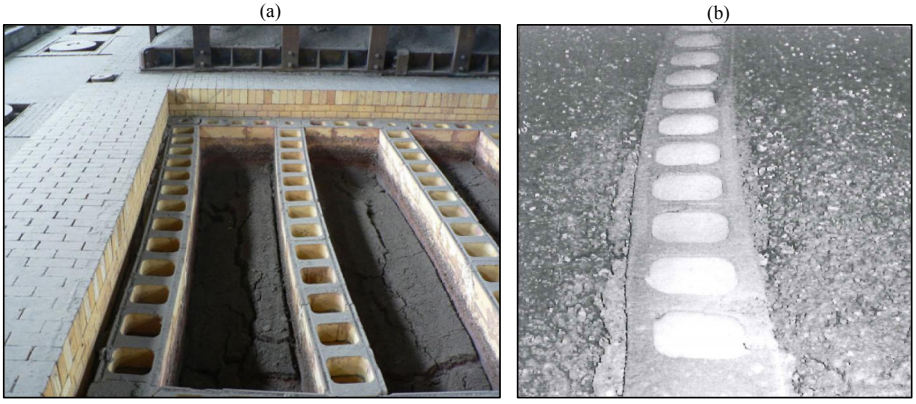

Figure 1. General view of (a) the flue wall deflection [11] and (b) Heavily slagged flue wall covered with metallurgical coke [10].

2. Model and computational method

2.1. Geometry model

A three-dimensional model was built comprising a typical baking furnace firing section between the centerline of a flue and the centerline of a pit. In the pit, 14 anodes of 1600 x 600 x 800 mm size are placed. There are 2 domains, a solid domain composed of flue wall, packing coke and anodes, and a fluid domain for the gas flow. The thickness of the solid domain material layers, flue wall, packing coke and anodes in the direction of the pit length is 100 mm, 100 mm and 300 mm, respectively. Symmetry was assumed on the centerline of the

flue and the pit.
This model is applied to the firing section of the furnace in order to explore the effect of the flue wall deformation on the anode baking quality and temperature distribution homogeneity. To reduce the computational cost, the combustion process is simulated using a simplified hot air jet model in this study. This is a widely used simplified approach, in which the combustion process and its thermal energy released are modeled by considering by an inlet of hot air [1]. In order to inject an amount of energy at the burners inlets equivalent to that injected with natural gas, the following strategy is used: The air is injected at the same temperature as the maximum flame temperature.
The flue wall deflection modes investigated in this study is the C shape convex, the deformation modes are presented in Fig. 2. They are qualitatively consistent with the flue wall deformation patterns (Figure. 1.). The present study can also provide useful insights on temperature distribution adjustment as a function of the flue wall and furnace design.

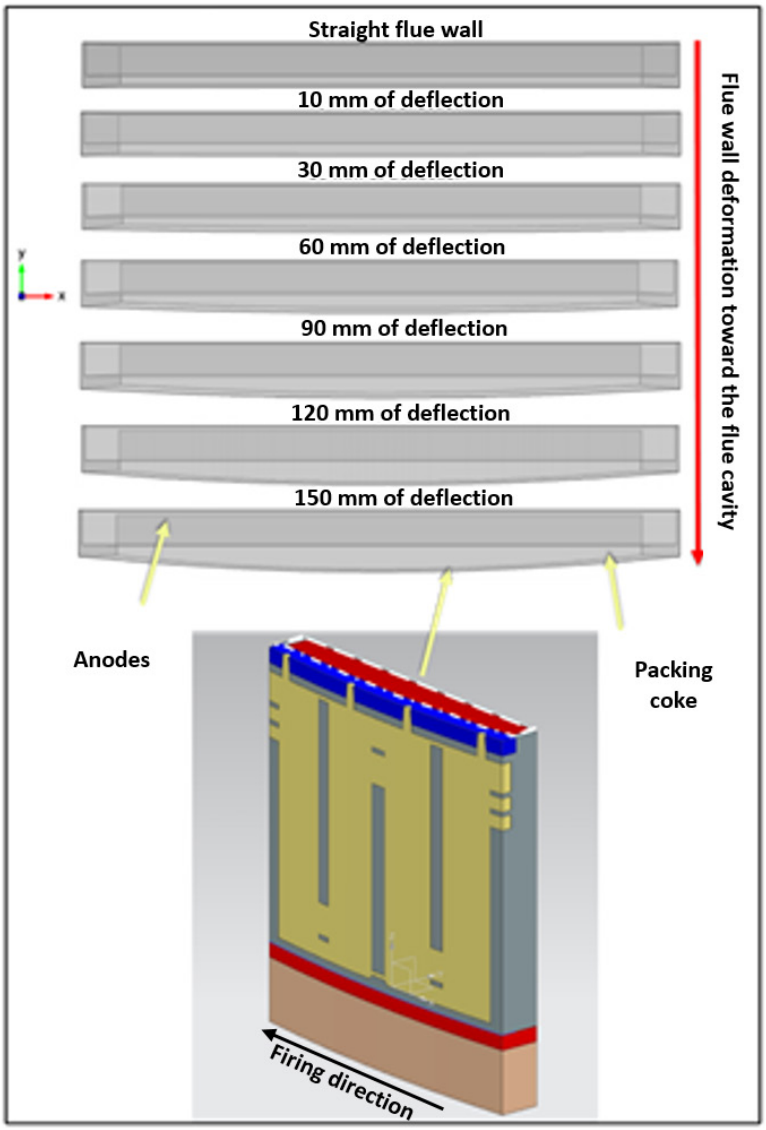

Figure 2. Schematic representation of the domains that is considered in the present study

2.2. Multiphysics mathematical model

In this work, we present a numerical framework that couples fluid, heat transfer. The numerical model was developed using the CDF commercial code COMSOL. Figure 3 shows an overview of the model of the baking furnace with an entire pit (solid domain) and the adjacent flues (gas flue domains). Phenomena that occur in the two parts of the furnace (solids and gas) are different so specific equations are solved in each part of the model through a virtual numerical interface. Thus, the global model of a baking furnace is divided into two sub-models: gas and pit (brick wall, packing coke, and anodes).

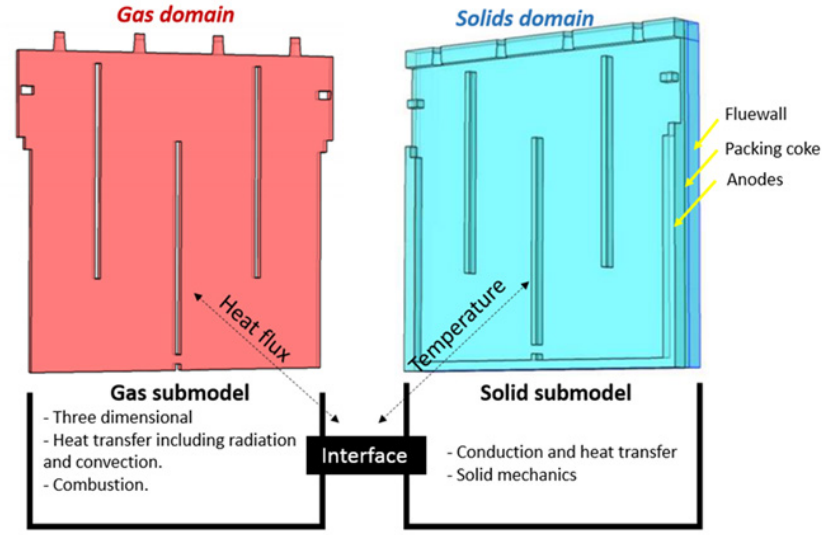

Figure 3. A schematic view of the flue and pit sub-models and their coupling.

These sub models are developed separately and then coupled through an interface at the flue wall surface on the flue side. This modular approach makes it easier to develop and modify each part. Also, if needed, each sub-model could be used exclusively for testing options in one part of the furnace (such as the flow distribution in the flue for a given geometry).On the gas part (flue), the flow, heat transfer and mass transfer equations are solved. On the solid part, the heat transfer by conduction is solved, considering the thermal conductivity of various solids (flue wall, packing coke and the anodes). The model is steady state and calculates for one heating section.

In an anode baking horizontal flue ring furnace, the temperature distribution is one of the key factors influencing the quality of baked anodes and is closely correlated with the gas flow [12, 13]. To understand the gas flow distribution in the flue, Navier-Stokes equations with turbulence model is adopted. The descriptions of incompressible gas flow are given as follow [14]:

$$\rho_g \nabla.\left(\boldsymbol{u}_g\right) = 0 \tag{1}$$

$$\rho_g \frac{\partial u_g}{\partial t} + \rho_g (\boldsymbol{u_g}.\nabla)\boldsymbol{u_g} = \nabla.[-p\overline{\boldsymbol{I}} + (\mu + \mu_T)(\nabla \boldsymbol{u_g} + (\nabla \boldsymbol{u_g})^T)] \tag{2}$$

$$\rho_g \frac{\partial \boldsymbol{k}}{\partial t} + \rho_g \left(\boldsymbol{u_g}\ .\nabla\right)\boldsymbol{k} = \nabla.\left[\left(\mu + \frac{\mu_T}{\sigma_k}\right)\nabla \boldsymbol{k}\right] + p_k - \rho_g \dot{\boldsymbol{o}} \tag{3}$$

$$\rho_g \frac{\partial \grave{o}}{\partial t} + \rho_g \left(\boldsymbol{u_g} .\nabla \right) \grave{o} = \nabla . \left[\left(\mu + \frac{\mu_T}{\sigma_{\grave{o}}} \right) \nabla \grave{o} \right] + C_{\grave{o}1} \frac{\grave{o}}{k} p_k - C_{\grave{o}2} \frac{\grave{o}^2}{k} \grave{o} \rho_g \tag{4}$$

where $\mu_T = C_\mu \rho_g \frac{k^2}{\grave{o}}$, $p_k = \mu_T \left[\nabla \boldsymbol{u} : \left(\nabla \boldsymbol{u} + \left(\nabla \boldsymbol{u} \right)^T \right) \right]$,

u_g refers to the gas velocity; k is the turbulent kinetic energy; ϵ the turbulent dissipation rate; p pressure; ρ_g denotes gas density; μ molecular viscosity; μ_T effective viscosity; σ_k and σ_ϵ are Prandlt number; p_k, $C_{\epsilon 1}$ and $C_{\epsilon 2}$ are constants [15].

Heat from the gas in the flue is transferred to the brick wall surface by convection and radiation, then by conduction from the flue wall surface into the bricks, and on to the packing coke, then the anodes. By combining Fourier's law and energy conservation law, the heat transfer through the solid can be represented in the following form, called transient heat conduction equation:

$$\rho_s C_p \frac{\partial \boldsymbol{T_s}}{\partial t} = \lambda_s \nabla \boldsymbol{T_s} - Q_s \tag{5}$$

T_s is the solids (anodes, packing coke and flue wall) temperature, and λ_s is the thermal conductivity. Q_s represents the thermal loss to the atmosphere by coke and the foundation, heat is exchanged by Radiation and convection following the relationship:

$$-n.\left(-\lambda \nabla \boldsymbol{T} \right) = \omega \sigma \left(T_\infty^4 - T^4 \right) + h_{equiv} \left(T_\infty - T \right) \tag{6}$$

At the brick wall surface, where solids and flue gases are in contact, heat is exchanged following the relationship:

$$q' = \left(h_C + h_R \right) \left(T_g - T_W \right) \tag{7}$$

where q' is the heat flux through the fluid-solid interface; h_c is the convection heat transfer coefficient between the flue wall and the gas; h_R is the radiation heat transfer coefficient between the flue wall and the gas flue; T_W is the flue wall temperature at the boundary; T_g is the gas temperature.

The convection heat transfer coefficient is determined by the Dittus-Boelter correlation [1]:

$$h_C = \left(\frac{\lambda_g}{D_h} \right) 0.023 \, Re^{0.8} Pr^{\gamma} \tag{8}$$

where λ_g is the thermal conductivity of gas; D_h is the representative hydraulic diameter inside the flue, Pr is Prandlt number of gas; γ is an exponent, Re is the Reynolds number of the flow.

The radiation heat transfer coefficient is given by [6]:

$$h_R = \sigma \left(\frac{w_g T_g^4 - \eta_g T_w^4}{T_g - T_W} \right) \tag{9}$$

where σ is the Stephan-Boltzmann constant= $5{,}67 \times 10^{-8}$ $[W.m^{-2}.K^{-4}]$; ω_g and η_g are the emissivity and the absorptivity of mixed gas, respectively.

As showed in Figure 4-a, at symmetry, the boundary conditions applied are:

- ✓ Heat transfer symmetric boundary conditions:

At symmetries, heat flux equals zero.

$$-n.\left(-\lambda_S \, .\nabla \boldsymbol{T_s} \right) = 0 \tag{10}$$

- ✓ Fluid flow symmetric boundary conditions:

At symmetry, there is no flow normal to the symmetric boundary, mathematically this is means that we specify that,

$$\boldsymbol{u_g}.n = 0 \tag{11}$$

$$\nabla \boldsymbol{K}.n = 0, \quad \nabla \grave{o}.n = 0 \tag{12}$$

Where n is the normal vector pointing to the boundary outside, T_s is the solid temperature, u_g is the gas velocity.Viscosity are assumed to remain constant at values corresponding to air at the inlet at 800°C.Thermal conductivity and viscosity are assumed constant and as a function of temperature, in this study both cases are explored. As showed in Figure 4-b, mesh is constituted of about 83123 tetrahedral elements and 22662 Triangular elements. Consequently, the complete 3D mesh typically contains 100000 elements. A hot jet air approaches is considered to include the energy generated by the natural gas combustion in order to reduce the computational burden of simulating anode baking furnaces and simply replacing the burner by an inlet of hot air at -20 Pa. In order to inject an amount of energy at the burners inlets equivalent to that injected with natural gas, the following strategy is used: The air is injected at the same temperature as the maximum flame temperature (1800°C). Although this strategy does not provide any information in order to improve combustion efficiency and reduce natural gas consumption, but it is interesting to document the ability of this simple approach to provide realistic anode temperature evolution and predict anode variability with the help of the hot air jet model.

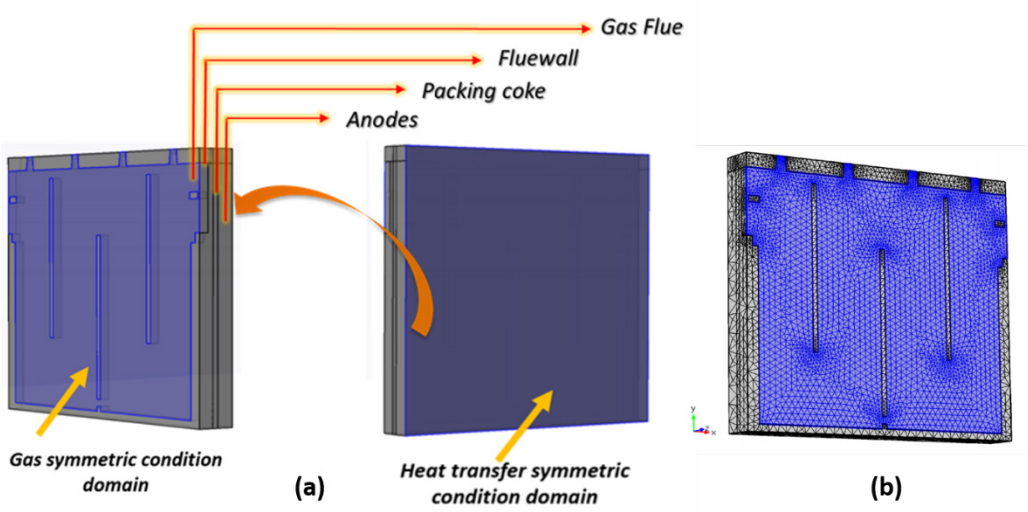

Figure 4. A schematic representation of (a) the model domain if symmetry could be assumed, (b) the domains meshing that is considered in the present study.

In this study, the solid thermal conductivity and specific heat (anodes and packing coke) are assumed varying as a function of the temperature, based on experimental data.. The Table 1summarizes the materials properties used in this study.

Table 1. Material properties used in this study.[1]

Materials properties as a function of temperature

Materials	Temperature (C)	Thermal conductivity ($W.m^{-1}.K^{-1}$)	Specific heat ($J.Kg^{-1}.K^{-1}$)	Density (Kg/m^3)
Flue wall		1.46	965	2490
Packing coke	20	0.87	652	1240
	100	0.87	941	
	300	0.95	1374	
	500	1.08	1650	
	700	1.24	1816	
	1000	1.50	2000	
Anodes	20	2.55	871	1545
	200	2.45	1105	
	500	3.75	1291	
	700	4.55	1311	
	850	5.30	1414	
	1000	6.05	1519	
	1200	7.00	1700	

Constant material properties

Materials	Thermal conductivity ($W.m^{-1}.K^{-1}$)	Specific heat ($J.Kg^{-1}.K^{-1}$)	Density (Kg/m^3)
Flue wall	1.46	965	2490
Packing coke	1.27	1822	1240
Anodes	5.33	1447	1545

3. Results and discussions

3.1. Straight flue wall

This model is applied to the firing section of the furnace in order to explore the effect of the flue wall deformation on the anode baking quality and temperature distribution homogeneity. Figure 5. a presents the flow pattern on the symmetry plane in the flue domain (the middle of the flue) for an air inlet velocity and a fuel inlet injection velocity of 2.5 m/s and of 10 m/s. As can be clearly seen, the fluid flow streamlines inside a flue cavity depends on the baffles position inside the flue wall. The flue geometry has a significant impact on the flow field. The baffles create low-velocity zones behind them due to the recirculation of flow. The flow distribution through the cavity thickness shows that there is a poor flow distribution zone behind the baffles (Dark blue-colored zones) and very high flow distribution zone (Light green-colored zones), around 2 m/s and 5 m/s, respectively. Figure 5. b presents the resulting pressure field inside the flue cavity. The pressure drop across the flue is also important for the blower power requirement to circulate the gas. The resulting pressure drop value corresponding to the flue-wall geometry is 25 Pa.

Figure 6 presents the temperature distribution within the flue cavity and in the flue wall-flue cavity interface. Figure 6. a shows the hot air jet extended inside the flue channel. As can be clearly seen from the temperature mapping, the maximum temperature in the flue cavity is between 1500 and 1800 °C near to the burners inlet. The minimum temperature in the flue cavity is around 677 °C, the low temperature zones (dark blue zones) are between 677 and 850°C These zones are located near to the air inlet and corresponding to the poor flow distribution zone (Figure 5. a). The medium zone temperature (light blue zones) is between 850 and 1050°C and corresponding to the high flow distribution area near to the outlet.

Although, the heat transfer towards the flue wall has smoothed to some extent the temperature distribution on the flue wall-flue cavity interface (Figure 6. b), the hot spot present near to the burners in the flue cavity has smoothed from 1600°C in the flue cavity to 1300°C in the flue wall–flue cavity interface, the flue wall temperature distribution is more homogenous and ranged between 900°C and 1300°C. Although the difference between the flue wall maximum and minimum temperature is still significant.

Figure 7. shows the temperature contours at the anodes middle-plane (Figure 7. a) and at the anodes-packing coke interface (Figure 7. b). As could be expected from the temperature contour at the flue wall-flue cavity interface (Figure 6. b), the warmest zones in the anode-packing coke interface is located at the top of the pit near to the outlet corresponding to the high temperature zone in the flue wall (Figure 6. b) and to the high flow distribution zone (Figure 7. a), the maximum temperature in the hot spot is around 1025 °C. The low temperature zone is located near to the inlet and the coldest zone near to the anode top surface, the low temperature zone is ranged between 825°C and 716°C. Moving from the packing coke-anode interface to the anode middle-plane (Figure 7. b), the heat diffusion in the solids has smoothed further the hot and cold spots present in the flue wall and the packing coke, as expected, the hot spot in the anode middle-plane is located near to the outlet and the temperature is around 925°C.

Except of the hot spot in the anodes located in a very narrow zone near to the second burner position, the anode temperature distributions is homogenous. The anode volume average temperature is around 891°C.

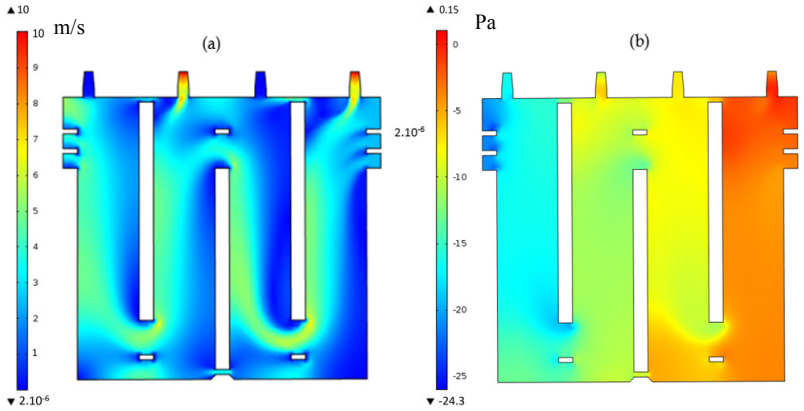

Figure 5. The flow pattern on the symmetry plane in a flue (the middle of the flue) and (b) the pressure distribution inside the flue cavity

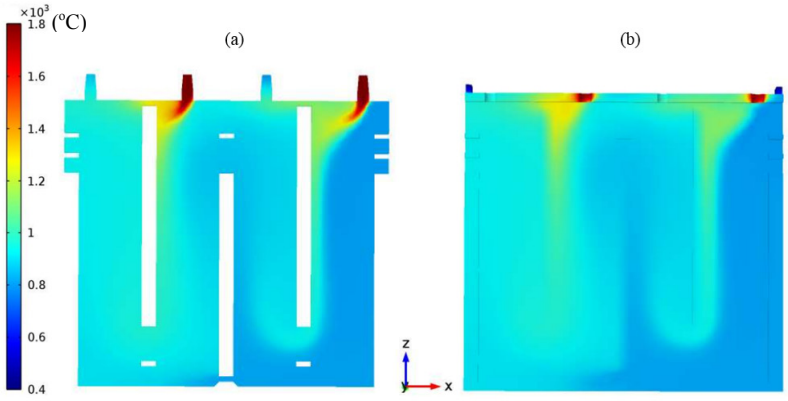

Figure 6. Temperature mapping distribution at (a) flue cavity and (b) the flue wall-cavity interface

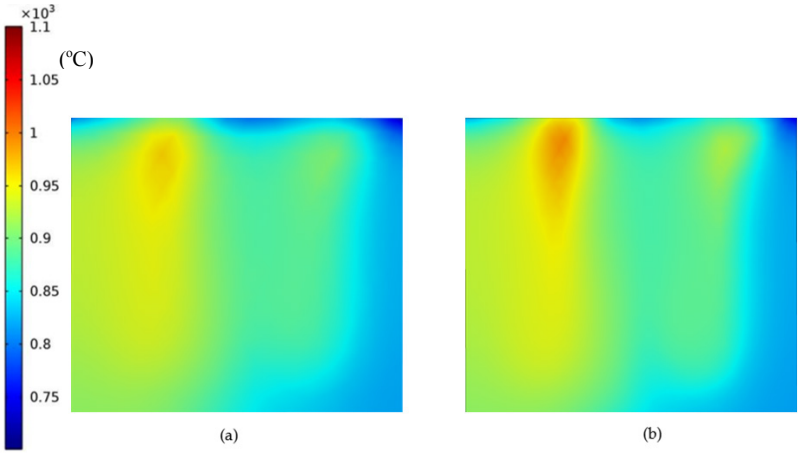

Figure 7. Anode map temperature at (a) the middle plane and (b) the packing coke interface.

3.2. Deformed flue wall - convex

The main purpose of this section is to explore the application of the thermo-hydro-mechanical model considering different modes of flue wall deformation for convex shape deformation toward the width of the flue cavity from a 0 mm of deflection for a straight a flue-wall to a 150 mm deflected flue wall (10, 30, 60, 90, 120 and 150 mm). 150 mm deformation mode is studied for comparison purposes and considering that the width of the half of the cavity is around 170 mm.

Same conclusions for the convex deflected flue wall, a very slight variation in the flow and the pressure distribution can be observed as a function of the flue wall deformation, compared to a straight flue wall distribution results. Moving to the Anode temperature distribution at the packing coke interface (Figure 8. a) and at the anode middle plane (Figure 8. b) as a function of the flue wall deflection. It can be clearly observed that the anode-packing coke and the anode middle plane temperature is decreasing by the increase of the flue wall deflection toward the flue cavity, through the cooling of the warm area and the hot spots and an under-baking of the cooler area.

This temperature evolution as a function of the flue wall deflection can be explained by the changing packing coke additional thickness between the flue wall and the anodes as a function of the convex flue wall deflection. From these results, it can be concluded that the packing coke have a very important role in protecting the anodes against air burn-from oxidizing gases and guarantee an efficient heat transfer from flue walls to anodes.

The anode temperature is decreasing by the increase of the flue wall deformation. For the packing coke-anode interface (Figure 8. a), the interface average temperature is around 892°C for a straight flue wall and decrease to reach 878°C for a 150 mm deflected flue wall. Moving from the packing coke-anode interface to the anode middle-plane (Figure 8. b), the heat diffusion in the solids has smoothed further the hot For the anode middle plane, the middle plane average temperature is around 890 °C for a straight flue wall, it decreases to reach 875°C for a 150 mm deflected flue wall.

The anode maximum temperature is decreasing from 992°C to 941°C for a straight flue wall and a 150 mm deflected flue wall respectively. The more the flue wall is deflected, the lower is the anode temperature leading to an under-baking of the cooler parts of the anodes and consequently to an inhomogeneous anodes baking. The homogeneity of the temperature can be presented by the range of temperature (the difference between the maximum and the minimum temperature of the anode), the range presented in Table 3 clearly shows that the range is decreasing from 275°C for a straight flue wall to 251°C for a 150 mm deflected flue wall. More details about the anode temperature distribution as a function of the flue wall deformation modes is displayed in Table 1.

Table 2. The anode temperature at the packing coke interface and the anode middle plane as a function of the flue wall deflection (C shape convex).

Anode temperature distribution	Case 1 (0 mm)	Case 2 (10 mm)	Case 3 (30 mm)	Case 4 (60 mm)	Case 5 (90 mm)	Case 6 (120 mm)	Case 7 (150 mm)
Maximum temp (°C)	992.3	983.4	973.2	966.5	953.2	947.9	941.6
Minimum temp (°C)	716.8	713.4	710.9	705.6	700.0	694.6	690.8
Max- Min (°C)	275.5	269.9	262.3	260.9	253.2	253.3	250.7
Volume average temp (°C)	891.1	888.3	887.0	885.6	881.9	879.4	876.5
Average temp (°C) PC-Anode interface	892.3	889.5	888.5	886.7	883.1	880.6	877.9
Average temp (°C) Middle- plane	889.9	887.2	885.9	884.3	880.7	878.1	875.2

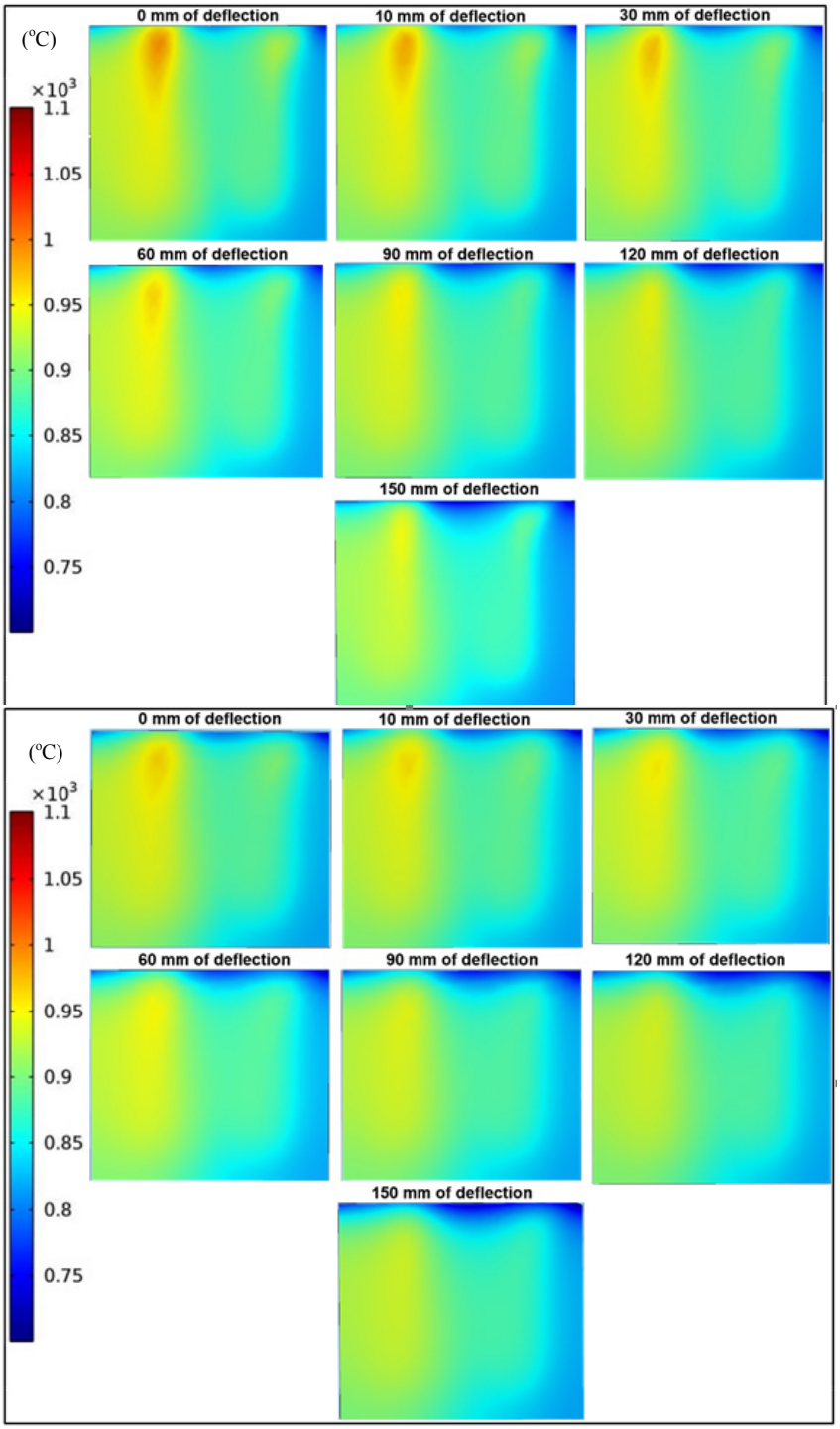

Figure 8. Anode map temperature at the packing coke interface (a) and the anode middle plane (b) as a function of the flue wall deflection (C shape convex deformation).

Figure 9. a shows the evolution of the Anode average temperature, at the anode middle plane and at the anode-packing coke interface as a function of the flue wall deflection, 0, 30, 60, 90, 120 and 150 mm deflected flue wall. It can be observed that the anode volume average temperature is decreasing by the increase of the flue wall deflection from 891°C to 876.5°C, for a straight and a 150 mm deflected flue wall, respectively.

Figure 9. b depicts the anode volume average, minimal and maximal temperature as a function of the flue wall deflection, the anode maximum temperature is decreasing from 992°C to 941.6°C for a straight flue wall and a 150 mm deflected flue wall, respectively. The anode minimum temperature is decreasing from 716.8°C to 691°C for a straight flue wall and a 150 mm deflected flue wall, respectively. The homogeneity of the temperature can be presented by the range of temperature, the range is decreasing from 275°C for a straight flue wall to 250.7°C for a 150 mm deflected flue wall leading to an inhomogeneous anodes baking.

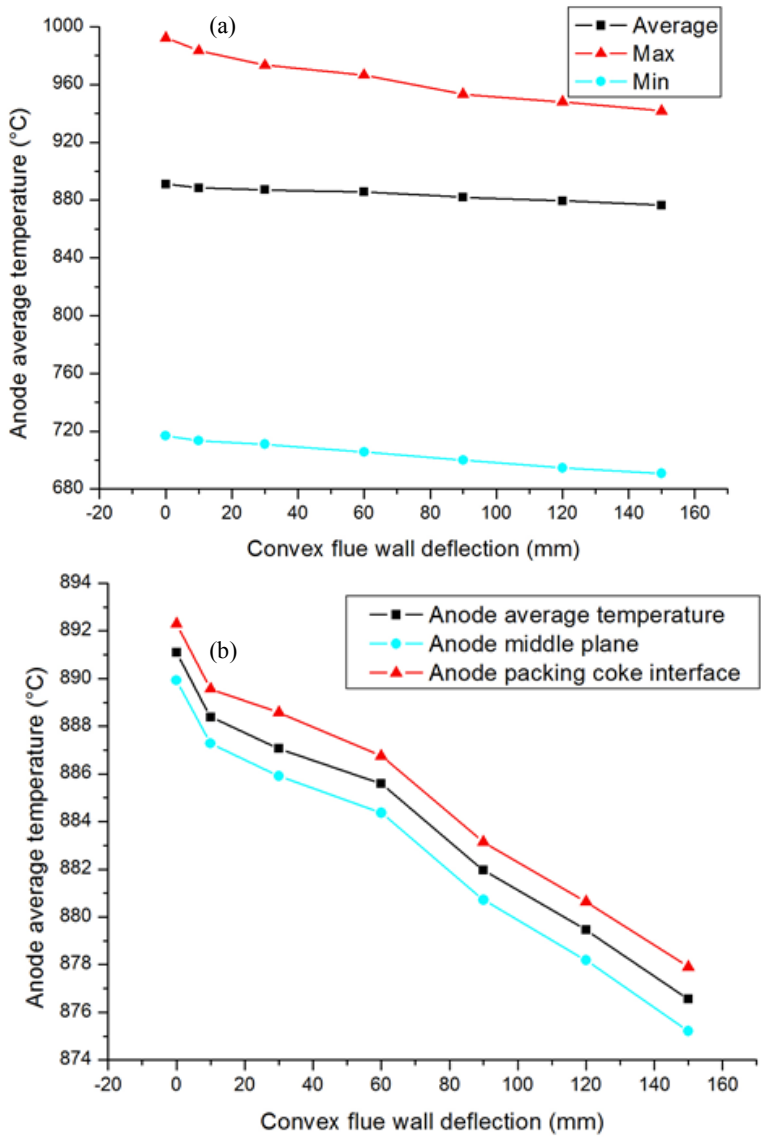

Figure 9. Anode map temperature at the packing coke interface (a) and the anode middle plane (b) as a function of the flue wall deflection (C shape convex deformation).

4. Conclusions

Flue-wall's aging is usually accompanied by its deformation. Such deformations create difficulties in loading and unloading anodes in the pits and to inhomogeneous anode baking. In this work, we developed a tool that can predict the anode temperature distribution, creation of hot spot and anode overbaking in certain area as a function of the flue wall deformation mode. Considering the anode temperature distribution for a straight flue wall as a reference case, the deflection of the flue wall C shape convex affect the anode baking temperature distribution and homogeneity and leads to an under-baking or an overbaking of the anode in certain area. Sometimes, the flue wall deflection leads to a redistribution of the anode temperature based on the original anode temperature distribution for a straight flue wall and on the degree and the shape of the flue wall deflection. Therefore, the expected anode temperature distribution and homogeneity for a deflected flue wall depends on the temperature distribution for a straight flue wall before deflection.

In the future, other flue wall deformation modes will be studied, the main purpose is to explore all the realistic flue wall deformation patterns, and how it affects the anode baking homogeneity, in order to establish a flue wall deformation modes database linked to the consequence on the anode baking quality.

Acknowledgements

This research paper is made possible through the help and support from the Emirates Global Aluminium (EGA). We are also very thankful for the carbon anode area representatives at EGA for providing the needed support.

References

1. F. Grégoire, L. Gosselin, H. Alamdari, Combustion in anode baking furnaces: Comparison of two modeling approaches to predict variability, *The Combustion Institute - Canadian Section, Spring Technical Meeting, At Québec City*, Québec, Canada 2013 338-343.
2. D.S. Severo, V. Gusberti, E.C. Pinto, Advanced 3D modelling for anode baking furnaces, *The minerals, Metals and Materials society (Light metals)* (2005) 697-702.
3. F. Goede, Refurbishment and modernization of existing anode baking furnaces, *Light metals, The minerals, Metals and Materials society* (2007) 973-976.
4. M. Baiteche, D. Kocaefe, Y. Kocaefe, D. Marceau, B. Morais, J. Lafrance, Description and Applications of a 3D Mathematical Model for Horizontal Anode Baking Furnaces, *Light Metals 2015, John Wiley & Sons, Inc*.2015, pp. 1115-1120.
5. Y. Kocaefe, M. Baiteche, N. Oumarou, D. Kocaefe, D. Marceau, B. Morais, Different mathematical modelling approaches to predict the horizontal anode baking furnace performance.
6. F.P. Incropera, D.P.D. Witt, Fundamentals of Heat and Mass Transfer, *4th Edition, Chapter 9*, 1996.
7. C. Allaire, Effect of the type of brick and mortar on the resistance to deflection of the flue walls in horizontal flue carbon furnaces, *Light Metals* (1994) 551-564.
8. P. Quirmbach, Rheinisch-Westfaelische Technische Hochschule, RWTH Aachen, (30 August 1994).
9. F. Brunk, Corrosion and behaviour of fireclay bricks used in the flues of open anode baking furnaces, *The Minerals, Metals & Materials Society, Light Metals* (1995) 641-646.

10. H. Lenz, F. Brunk, Improved anode baking furnace cover material, *Light Metals* (2002) 629-632.
11. A. Yurkov, Refractories for Aluminium, Switzerland, (2015) 245-249.
12. P. Zhou, C. Mei, J.-m. Zhou, N.-j. Zhou, Q.-h. Xu, Simulation of the influence of the baffle on flowing field in the anode baking ring furnace, *Journal of Central South University of Technology* 9(3) (2002) 208-211.
13. T.W. Quan, Numerical Heat Transfer, Xi'an Jiaotong University Press: Xi'an1988, p. 220−231.
14. F. Jian-ren, Q. Ke-fa, Theory and Calculation of Gas-solid Multi-phase Flow in Engineering [M]. *Hangzhou: Zhejiang University Press* (in Chinese) (1989).
15. D.S. Severo, V. Gusberti, User-friendly software for simulation of anode baking furnaces. , *Proceeding of the 10th Australasian Aluminum Smelting Technology Conference*, 2011.